TUST 924
17 November 2005; Disk Used
ARTICLE IN PRESS
No. of Pages 9, Model 5+

Available online at www.sciencedirect.com
SCIENCE DIRECT®

Tunnelling and Underground Space Technology xxx (2005) xxx–xxx

Tunnelling and Underground Space Technology
incorporating Trenchless Technology Research

www.elsevier.com/locate/tust

Dynamic response of lined circular tunnel to plane harmonic waves

M. Esmaeili *, S. Vahdani, A. Noorzad

Faculty of Engineering, Department of Civil Engineering, University of Tehran, No. 137-Mehr Buildings, Boulvar Shahid Akbari, Azadi Street, Tehran, Iran

Received 21 October 2004; received in revised form 1 August 2005; accepted 15 October 2005

Abstract

Two dimensional harmonic response of lined circular tunnels in elastic full space medium against plane P–SV waves is investigated. The solution uses hybrid boundary, and finite element methods for modelling of media and lining, respectively. In the proposed ring element used in modelling of lining, the radial and tangential deformations are defined by Fourier series expansion. Therefore, the direct finite element unknowns of the problem are introduced as coefficients of these series. The non-dimensional shear and hoop stresses in the lining, and the same parameters in its interface with surrounding media are presented.

Keywords: Lined circular tunnel; Hybrid formulation; Ring element

1. Introduction

The internal forces and stress concentration in lining of tunnels due to earthquake waves are considered to be important design parameters. It is believed that these structures experience a lower rate of damage comparing to surface structures. However, failure of several underground structures during recent earthquakes proposes a deeper consideration in detail design of these structures. Among various phenomena happening to the lining of tunnels by earthquake waves, the distortion of cross section or ovalization phenomenon has the major effect (St. John and Zahara, 1987; Wang, 1993; Kim and Konagai, 2000; Hashash et al., 2001). Ovaling or racking deformation in a tunnel structure is developed when shear and pressure waves propagates normal, or near to normal, to the tunnel axis and results in distortion of cross sectional shape of tunnel lining. In addition, as far as the internal forces in lining are concerned, the lower modes of ovalization have the most participation in the lining deformations. Referring to the available solutions in the literature, expanding the ovalization modes in Fourier series, choosing the proper terms as are shown in Fig. 1, and considering the series' coefficients as variational constants in functional formulation, is properly used where the effect of cross sectional deformations are to be considered in pipe and elbow elements (Bathe et al., 1980,1982,1983).

From other point of view, where the wave propagation through the cavities is concerned, there are three major methods for analysis of the wave scattering. Method of wave function expansion, method of integral equation, and method of integral transforms (Pao and Maw, 1973).

Baron and Matthews (1961) investigated the diffraction of pressure wave by cylindrical cavity in an elastic medium using integral transform technique.

Pao and Maw (1973) studied wave diffraction around a cylindrical cavity in an infinite medium using wave function expansion. Lee (1977) used complex variable solution for incident SH wave to cylindrical cavity. In the other study, Achenbach and Kitiahara (1986) studied the reflection and transmission of an obliquely incident plane wave by array of spherical cavities by superposition of an infinite number of wave modes. Karl and Lee (1991) used a general method for study of SH wave scattering by underground cylindrical cavity. Deformation near circular underground cavity subjected to P wave was investigated in the form of Fourier Bessel series by Lee and Karl (1993). Other studies

* Corresponding author. Tel.: +98 21 88095417; fax: +98 7607090.
E-mail address: moresm76@yahoo.com (M. Esmaeili).

0886-7798/$ - see front matter © 2005 Published by Elsevier Ltd.
doi:10.1016/j.tust.2005.10.002

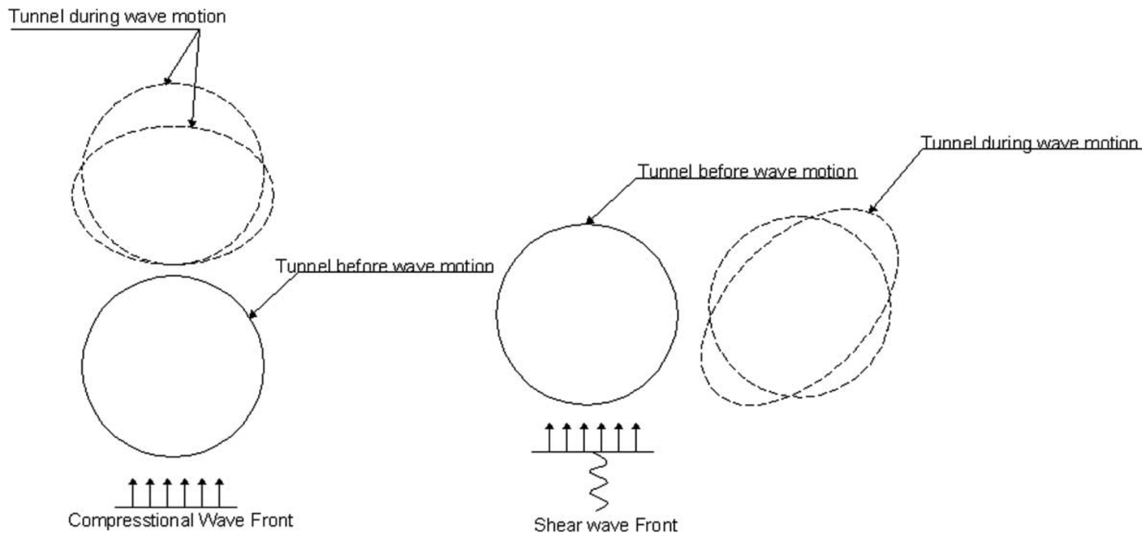

Fig. 1. Ovaling of circular tunnel due to seismic wave motion.

in similar manner had been done by Lee and Cao (1989) and Cao and Lee (1990) and Lee and Karl (1992) in two dimensional study of plane elastic waves scattering.

In the case of lined tunnel or embedded pipelines, the number of problems of wave diffraction under condition of plane strain has been solved using analytical and numerical methods such as FEM, BEM or FEM/BEM.

Lee and Trifunace (1979) obtained an analytical solution for response of underground circular tunnel to incident SH-waves. In plane strain condition, EL-Akily and Datta (1980, 1981) presented two methods of mach asymptotic expansion and successive reflection for steady-state response of circular cylindrical shell in half space. Hwang and Lysmer (1981) used a special FEM in frequency domain for dynamic analysis of buried structures to plane travelling wave. Datta and Shah (1982) have undertaken a study on wave scattering around single or multiple cavities. Shah et al. (1982, 1983) have presented two-dimensional results for wave scattering by single and multiple scatterers.

Wong et al. (1985) used a hybrid finite element method and wave function expansions to study scattering at an inclusion. Kontoni et al. (1987) and Luco and De Barros (1994) have presented additional results for SH, P, SV and Rayleigh waves and conducted a detailed comparative study with previous two-dimensional solutions. Khair et al. (1989) and Liu et al. (1991) describe a frequency domain FEM/BEM in conjunction with a half space Green's function and Zhang and Chopa (1991a,b,c) explain a direct frequency domain BEM in conjunction with the full space Green's function for seismic analysis of tunnels. Stamos and Beskos (1996) have used BEM for study of 3D seismic response of long lined tunnels in half-space. Moore and Guan (1996) investigated the three-dimensional response of a pair of lined cylindrical cavities located in full-space subject to incident seismic waves by method of successive reflections and transforming co-ordinate systems for the wave function expansions.

In recent developments, a combination of boundary element method with a plane finite element mesh for modelling of the lining at the boundary of the cavity is used to achieve the lining internal forces.

The method is limited to two dimensional analysis and is considered costly, since the flextural behaviour of lining is modelled using plane strain elements.

In the present work, a FEM/BEM method is chosen, but the behaviour of lining is replaced by introducing a ring element, with the same concept of ovalization used in elbow element (Bathe et al., 1980,1982,1983; Vahdani, 1982). In this way, not only the flextural behaviour of lining is modelled using a few modes of Fourier series, but the analysis can be extended to the longitudinal direction, useful for analysis of curved tunnels. Of course the method is limited to circular tunnels.

2. Boundary element formulation of wave scattering around circular cavities

For elastic, homogeneous, isotropic domain Ω, the equations of motion or Navier's equations are presented as:

$$\mu u_{i,jj} + (\lambda + \mu) u_{j,ji} + \rho b_i = \rho \ddot{u}_i, \tag{1}$$

where λ and μ are Lame's constants and ρ is medium density.

Denoting pressure and shear wave velocities by c_1 and c_2, respectively, Eq. (1) can be re-written in frequency domain with its corresponding boundary conditions:

$$(c_1^2 - c_2^2) u_{i,ij} + c_2^2 u_{j,ii} + b_j + \omega^2 u_j = 0, \tag{2}$$

$$u_i(x,\omega) = U_i \quad : x \in \Gamma 1, \tag{3}$$

$$t_i(x,\omega) = \sigma_{ij} n_j = T_i \quad : x \in \Gamma 2,$$

where T_i and U_i are the traction and displacement vectors, respectively, and $\Gamma = \Gamma_1 + \Gamma_2$ represents the surface of the domain.

The weak form of Eq. (2), using displacement and traction fundamental solutions, and reciprocal theorem in elastodynamic can be written as follows:

$$u_l^i + \int_\Gamma p_{lk}^* u_k \,\mathrm{d}\Gamma = \int_\Gamma u_{lk}^* p_k \,\mathrm{d}\Gamma, \tag{4}$$

where u_{lk}^* and p_{lk}^* are the displacement and traction in k-direction, when the load is applied in the l-direction.

u_k, p_k are displacement and traction in boundary points. Moving the loading point to boundary and omitting created singularities, the other form of above equation is

$$c_{lk}^i u_k^i + \int_\Gamma p_{lk}^* u_k \,\mathrm{d}\Gamma = \int_\Gamma u_{lk}^* p_k \,\mathrm{d}\Gamma, \tag{5}$$

where the coefficients c_{lk}^i are equal to $\frac{1}{2}\delta_{lk}$ for any point on the smooth boundary. Using isoperimetric quadratic elements for discretization of the cavity's boundary, the matrix representation of Eq. (5) is

$$c^i u^i + \sum_{j=1}^{NE} \left\{ \int_{\Gamma_j} p^* \Phi \,\mathrm{d}\Gamma \right\} u^j = \sum_{j=1}^{NE} \left\{ \int_{\Gamma_j} u^* \Phi \,\mathrm{d}\Gamma \right\} p^j, \tag{6}$$

$$\Phi = [\Phi_1, \Phi_2, \Phi_3], \tag{7}$$

$$\Phi_K = \begin{bmatrix} \phi_k & 0 \\ 0 & \phi_k \end{bmatrix}, \tag{8}$$

where the ϕ_k are quadratic interpolation functions and NE is the number of boundary elements.

In Eq. (6), the integral along Γ_j needs to be transformed to the homogeneous coordinate as follow:

$$\int_{\Gamma_j} p^* \Phi \,\mathrm{d}\Gamma = \int_{-1}^{+1} p^* \Phi |G| \,\mathrm{d}\xi = \int_{-1}^{+1} p^* [\Phi_1 \Phi_2 \Phi_3] |G| \,\mathrm{d}\xi = [h_1^{ij} h_2^{ij} h_3^{ij}], \tag{9}$$

$$\int_{\Gamma_j} u^* \Phi \,\mathrm{d}\Gamma = \int_{-1}^{+1} u^* \Phi |G| \,\mathrm{d}\xi = \int_{-1}^{+1} u^* [\Phi_1 \Phi_2 \Phi_3] |G| \,\mathrm{d}\xi = [g_1^{ij} g_2^{ij} g_3^{ij}], \tag{10}$$

where $|G|$ is the Jacobin matrix and ξ is local coordinate along the boundary elements.

Assembling the element matrixes along the N boundary point will result in general matrix equation,

$$HU = GP, \tag{11}$$

where H and G are the $2N \times 2N$ square matrixes that contain integral of traction and displacement tensors as shown in Eqs. (9) and (10) (Dominguez, 1993).

In the case of P–SV waves scattering, total displacement and traction fields at the boundary of unlined tunnel are defined as:

$$u = u^i + u^s, \tag{12}$$

$$p = p^i + p^s = 0, \tag{13}$$

where u^i and u^s are incident and scattered wave displacement fields, and p^i and p^s are incident and scattered tractions, respectively. Having the applied incident wave displacement field u^i, the boundary displacements can be obtained by solving the matrix equation (11), in conjunction with Eqs. (12) and (13) (Manolis and Beskose, 1988).

3. Ovalization of the lining

The tunnel lining, as a separate structure, will experience some deformations by the earthquake wave passing through the media. Assuming that the lining will not be separated from the cavity, the boundary element formulation should include the strain energy stored in lining during earthquake deformations. Evaluation of this energy may be done by expanding the deformations of the lining in terms of Fourier series and choosing the proper terms as are shown in Figs. 2 and 3, and described by the following equations:

$$u_r = C_0 - C_1 \cos\theta + C_2 \sin\theta - 2C_3 \cos 2\theta + 2C_4 \sin 2\theta, \tag{14}$$

$$u_\theta = C_1 \sin\theta + C_2 \cos\theta + C_3 \sin 2\theta + C_4 \cos 2\theta. \tag{15}$$

As it can be seen, the term C_0 will explain uniform expansion of lining, the term C_1 and C_2 will cause no deformation, but allow the rigid body transformations and the terms C_3 and C_4 will explain the symmetric and asymmetric ovalizations, which are the major deformations components (Vahdani, 1982). Of course more terms can be added to the series if needed.

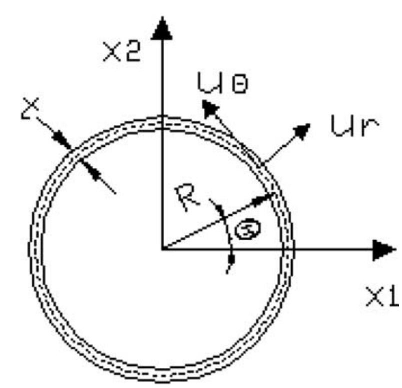

Fig. 2. Deformation field for circular tunnel lining.

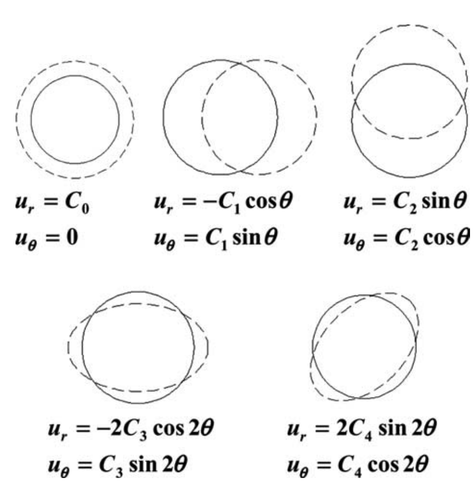

Fig. 3. Deformation modes of cavity.

The corresponding strain components for thin lining can be derived as follows (Oden and Ripperger, 1981):

$$\varepsilon_{\theta\theta} = \frac{u_r}{R} + \frac{1}{R}\frac{\mathrm{d}u_\theta}{\mathrm{d}\theta} - \frac{y}{R^2}\frac{\mathrm{d}^2u_r}{\mathrm{d}\theta^2}, \tag{16}$$

$$\gamma_{r\theta} = \frac{1}{R}\frac{\mathrm{d}u_r}{\mathrm{d}\theta}, \tag{17}$$

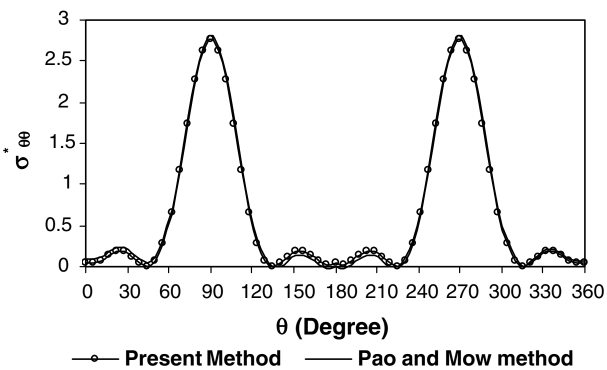

Fig. 4. Comparison of hoop stress around circular cavity for P wave with $\frac{\omega r}{c_1} = 1$ in present method with Pao and Maw Method (1973).

where, R is the mean radius of the lining.

Substitution of, u_r, u_θ from Eqs. (14) and (15) will result in the following matrix equation:

$$\varepsilon = B \cdot C^{\mathrm{T}}, \tag{18}$$

where

$$B = \begin{bmatrix} \frac{1}{R} & \frac{-y\cos\theta}{R^2} & \frac{y\sin\theta}{R^2} & \frac{-8y\cos 2\theta}{R^2} & \frac{8y\sin 2\theta}{R^2} \\ 0 & \frac{\sin\theta}{R} & \frac{\cos\theta}{R} & \frac{4\sin 2\theta}{R} & \frac{4\cos 2\theta}{R} \end{bmatrix}, \tag{19}$$

$$C = [C_0 \quad C_1 \quad C_2 \quad C_3 \quad C_4]. \tag{20}$$

In any variational approach, such as the Rayleigh–Ritz method, minimization of the potential energy will establish the equilibrium equation and lies to the appropriate stiffness matrix. In this case, the C constants only approximate the deformations of lining and are independent from other constants which explain the deformation of the media. Therefore, the above-mentioned minimization, will result in the stiffness of the lining, if it supposed to be loaded independently, or the lining's stiffness participation in its interaction with the deformations of media.

Forming the strain energy and handling the required integrals will lie to the following 5×5 stiffness matrix:

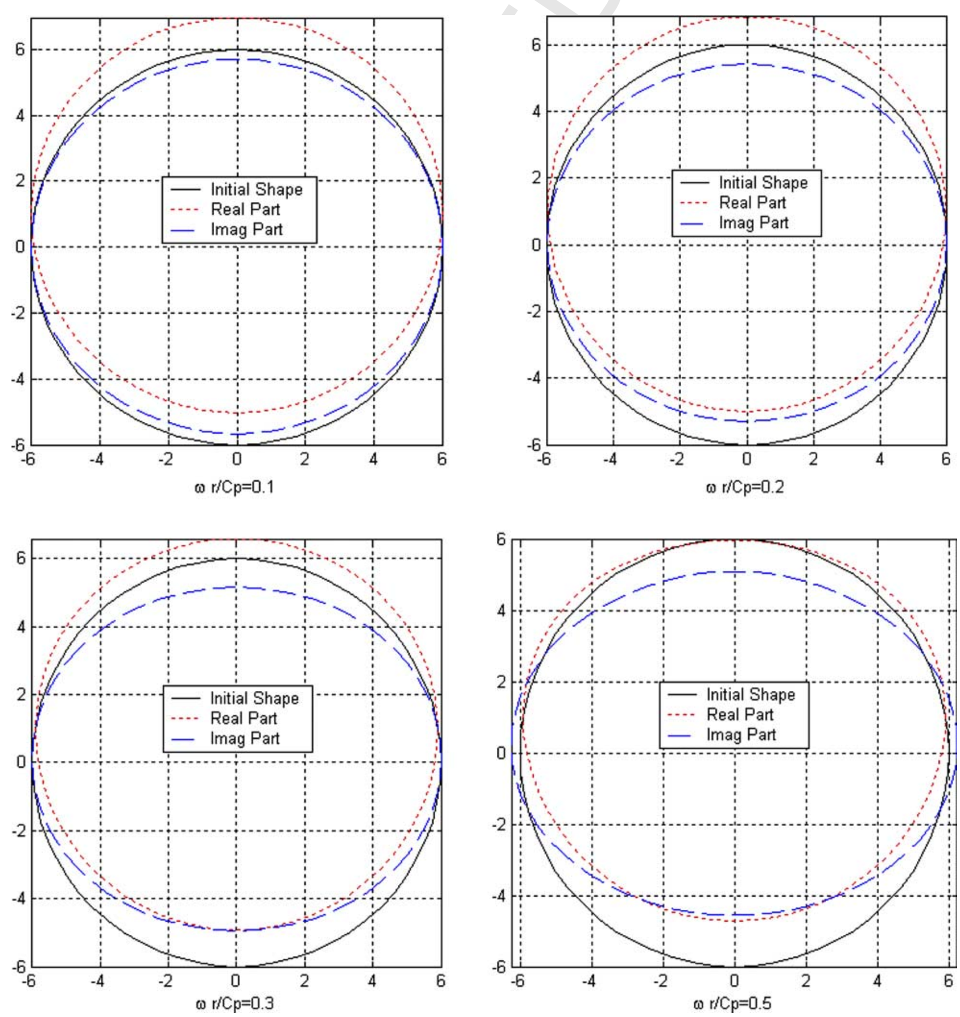

Fig. 5. Deformation components of cavity with radius equal to 6 m against vertical P wave.

$$\delta E = \frac{1}{2}\int_V (\varepsilon \cdot \sigma)\,\mathrm{d}V = \frac{1}{2}\int_V \varepsilon D \varepsilon\,\mathrm{d}V, \tag{21}$$

$$K_{\mathrm{RING}} = \int_{-\frac{t}{2}}^{\frac{t}{2}} \int_0^{2\pi} (B^{\mathrm{T}} \cdot D \cdot B) \cdot R\,\mathrm{d}\theta\,\mathrm{d}y, \tag{22}$$

$$D = \frac{E}{2(1+v)} \begin{bmatrix} 2(1+v) & 0 \\ 0 & 1 \end{bmatrix}, \tag{23}$$

$$[K]\{C\} = \{F\}, \tag{24}$$

where D is the matrix of constants and E and v are elasticity module and Poisson ratio of the ring material, respectively, and F is the 5×1 vector of external forces.

4. Mixed formulation

The interaction of the lining and media, under the effect of earthquake waves, may be established by equating the

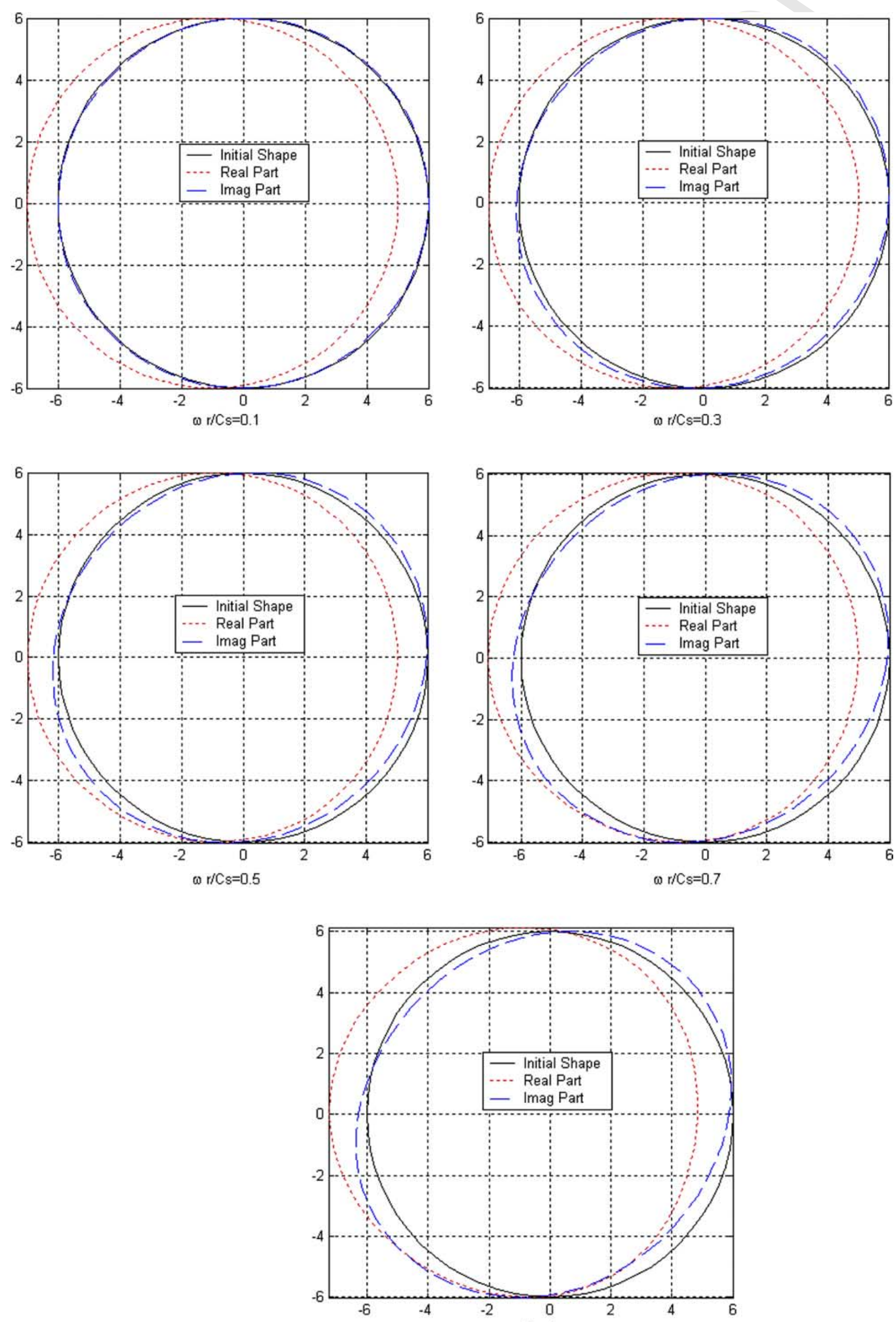

Fig. 6. Deformation components of cavity with radius equal to 6 m against vertical SV wave.

displacements of lining and the media at the cavity's boundary (Brebbia and Dominguez, 1989). Of course, these two fields of deformations have been estimated differently in the previous sections. Deformations of lining are expressed in terms of C constants, and the same deformations due to media are in terms of nodal displacements. Changing the BEM's deformations in terms of C constants, and equating them with the lining deformations will result in the final assembled equations as follow:

$$[M]_{2N\times 2N}[G]^{-1}_{2N\times 2N}[H]_{2N\times 2N}\{U^{\mathrm{S}}\}_{2N\times 1} = [M]_{2N\times 2N}\{P^{\mathrm{S}}\}_{2N\times 1}, \tag{25}$$

$$M = \int_{\Gamma} N^{\mathrm{T}} N \,\mathrm{d}\Gamma, \tag{26}$$

$$N = \begin{bmatrix} \phi_1 & 0 & \phi_2 & 0 & \phi_3 & 0 \\ 0 & \phi_1 & 0 & \phi_2 & 0 & \phi_3 \end{bmatrix}, \tag{27}$$

where ϕ_1, ϕ_2, ϕ_3 are quadratic interpolation functions.

Using the Eqs. (14) and (15) for N boundary points, the general transformation matrix could be established:

$$\{U^{\mathrm{S}}\}_{2N\times 1} = [T]_{2N\times 5}\{C^{\mathrm{S}}\}_{5\times 1}, \tag{28}$$

$$T_N = \begin{bmatrix} 1 & -\cos\theta_N & \sin\theta_N & -2\cos 2\theta_N & 2\sin 2\theta_N \\ 0 & \sin\theta_N & \cos\theta_N & \sin 2\theta_N & \cos 2\theta_N \end{bmatrix}, \tag{29}$$

where the $\{C^{\mathrm{S}}\}$ vector contains the soil–structure interaction effect. Substituting $\{U^{\mathrm{S}}\}$ from Eq. (28) in Eq. (25), will result,

$$T^{\mathrm{T}}\cdot M\cdot G^{-1}\cdot H\cdot T\cdot C^{\mathrm{S}} = T^{\mathrm{T}}\cdot M\cdot P^{\mathrm{S}}. \tag{30}$$

Adding the stiffness matrix of ring from Eq. (24) to the above equation, assuming F equal to zero, gives the final form of soil–structure interaction equation,

$$(K + T^{\mathrm{T}}\cdot M\cdot G^{-1}\cdot H\cdot T)\cdot C^{\mathrm{S}} = T^{\mathrm{T}}\cdot M\cdot P^{\mathrm{S}}. \tag{31}$$

Vector of constant $\{C^{\mathrm{S}}\}$ can be calculated from Eq. (31). Similarly for incident wave Eq. (28) may be written as:

$$\{U^i\}_{2N\times 1} = [T]_{2N\times 5}\{C^i\}_{5\times 1}, \tag{32}$$

$$\{C^i\} = ([T]^{\mathrm{T}}[T])^{-1}([T]^{\mathrm{T}}\{U^i\}). \tag{33}$$

Finally we have

$$\{C\} = \{C^i\} + \{C^s\}. \tag{34}$$

In the above equations, the vector U^i are the imposed wave displacements, and C constants are the unknowns to be found. In the next step, the hoop and shear stresses distributions around the ring could be evaluated.

5. Numerical examples

Three examples are presented to evaluate the proposed method, as well as to compare the results with other sources, where it is possible. In the first example, the aim is to verify the algorithm. Therefore, a cavity with no lining is chosen to be compared with results of analytical work done by Pao and Maw (1973). The hoop stress around the circular cavity caused by pressure wave with

Table 1
Characteristics of material in second example

Ratio of ring shear modulus to medium $\frac{\mu_r}{\mu_m}$	Ratio of outer radius of ring to inner radius η	Ring Poisson ratio	Medium Poisson ratio
3	1.05	0.25	0.25

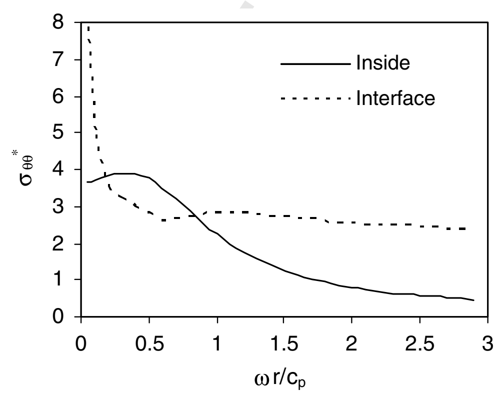

Fig. 7. Hoop stress at inside and interface of tunnel lining for vertical P wave.

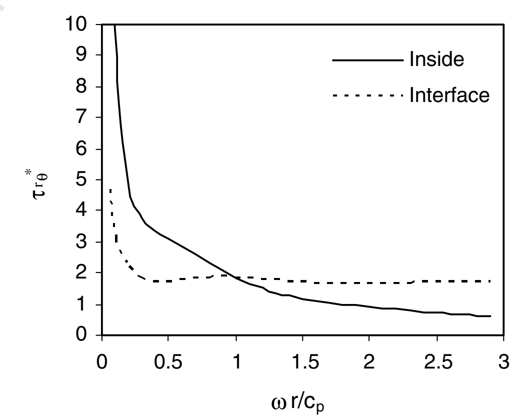

Fig. 8. Shear stress at inside and interface of tunnel lining for vertical P wave.

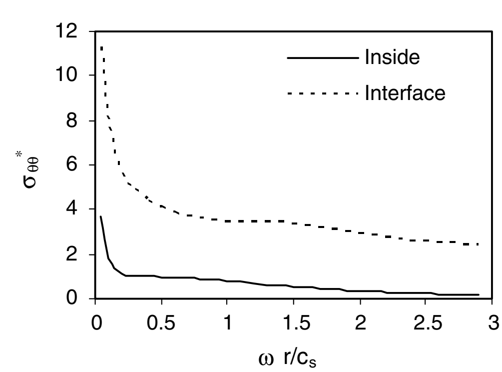

Fig. 9. Hoop stress at inside and interface of tunnel lining for vertical SV wave.

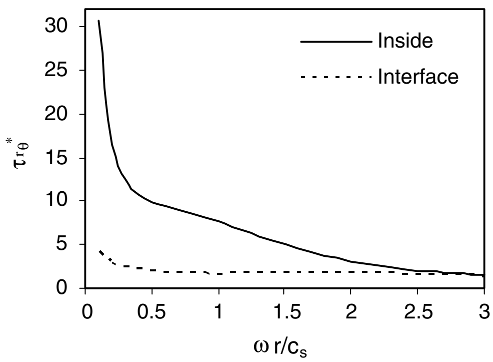

Fig. 10. Shear stress at inside and interface of tunnel lining for vertical SV wave.

non-dimensional frequency equal to one ($\frac{\omega r}{c_1}$, where ω is circular frequency, r is radius of cavity and c_1 is pressure wave velocity) is presented in Fig. 4, which shows the very good agreement with the above-mentioned work. Furthermore, the imaginary and the real parts of the solution for P and SV waves for various non-dimensional frequencies are shown in Figs. 5 and 6, which represents the rigid body and ovalization modes of deformation, respectively.

In the second example, a lining with the characteristics of Table 1 is added to the cavity.

The stresses concentration factors are shown in Figs. 7–10 for various non-dimensional frequencies of P and SV waves, respectively. In this example the hoop and shear stresses in the lining are presented non-dimensionally for inside and interface of lining and media, respectively.

In third example, the effect of thickness and relative shear modulus of medium to ring is investigated by a parametric study in non-dimensional frequency equal to 0.3. The characteristics of the material are shown in Table 2.

Table 2
Characteristics of material in third example

Ratio of medium shear modulus to ring $\frac{\mu_m}{\mu_r}$	Ratio of outer radius of ring to inner radius η	Ring Poisson ratio	Medium Poisson ratio
0.1 to 1.5	1.01, 1.05, 1.1	0.25	0.25

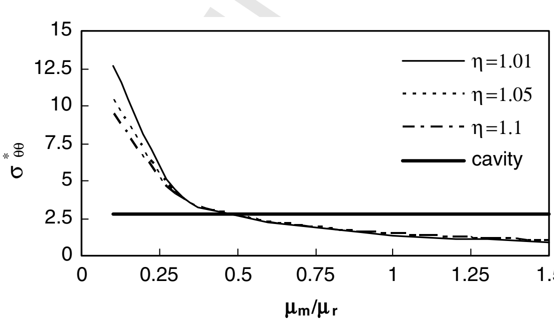

Fig. 11. Effect of thickness and shear modulus ratio on hoop stress at inside of tunnel lining for vertical P wave.

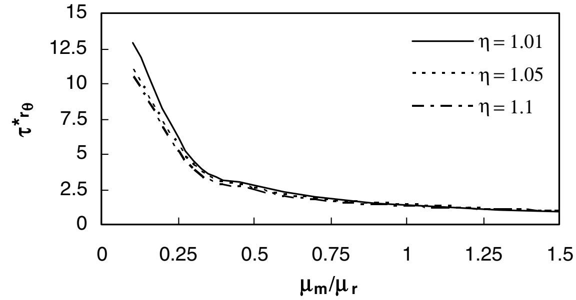

Fig. 12. Effect of thickness and shear modulus ratio on shear stress at inside of tunnel lining for vertical P wave.

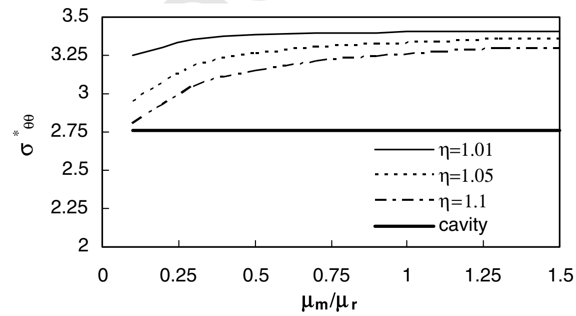

Fig. 13. Effect of thickness and shear modulus ratio on hoop stress at interface of tunnel lining for vertical P wave.

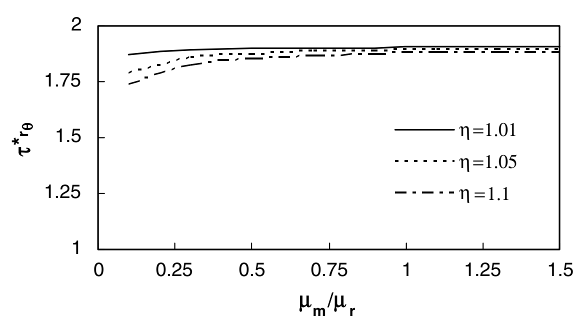

Fig. 14. Effect of thickness and shear modulus ratio on shear stress at interface of tunnel lining for vertical P wave.

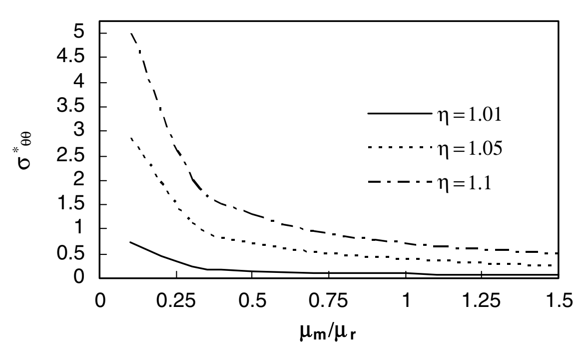

Fig. 15. Effect of thickness and shear modulus ratio on hoop stress at inside of tunnel lining for vertical SV wave.

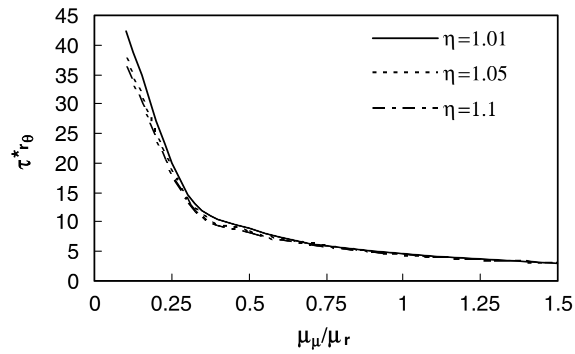

Fig. 16. Effect of thickness and shear modulus ratio on shear stress at inside of tunnel lining for vertical SV wave.

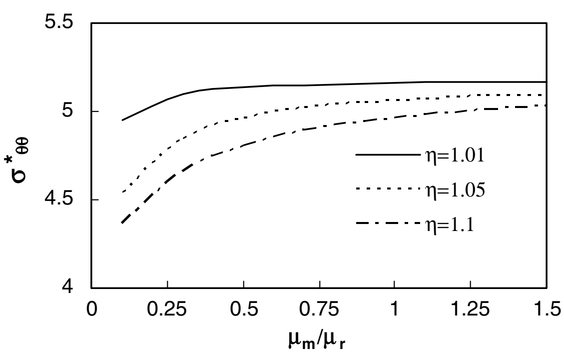

Fig. 17. Effect of thickness and shear modulus ratio on hoop stress at interface of tunnel lining for vertical SV wave.

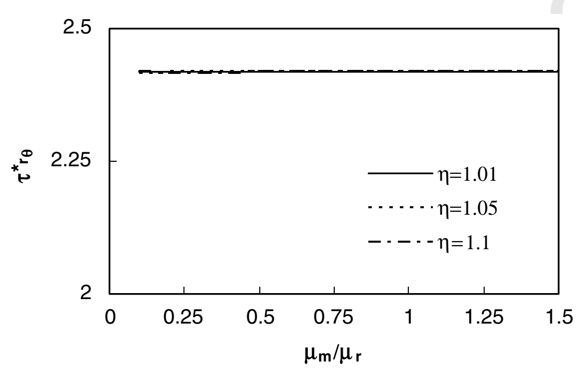

Fig. 18. Effect of thickness and shear modulus ratio on shear stress at interface of tunnel lining for vertical SV wave.

As it can be seen in Figs. 11–18, the increase in $\frac{\mu_m}{\mu_r}$ ratio or thickness, causes the reduction of stresses in lining. In addition in the case of SV wave and soft to very soft ring, variation of thickness does not have any effect on interface shear stress.

6. Conclusion

The stress concentration in circular tunnel linings has been studied, subjected to the seismic waves.

It is shown that trigonometric functions are very suitable to represent the deformations of circular tunnel lining in mixed formulation of FEM/BEM. Also the proposed method is expandable to the longitudinal direction, in the case of curved axis tunnel lining.

It is shown that for low frequency waves the rigid body transformation of the cavity due to wave passing is very well separated from deformations by the means of real and imaginary parts of the results. Therefore, the method can accurately be used with a few terms, since the deformations of cavity itself is very close to the ovalization, and more terms may be needed otherwise. Stiffness of lining does not change the maximum stress concentration, which occurs in non-dimensional frequency of 0.3.

References

Achenbach, J.D., Kitiahara, M., 1986. Reflection and transmission of an obliquely incident wave by an array of spherical cavities. J. Acoust. Soc. Am. 80 (4), 1209–1214.

Bathe, k.J., Almedia, C.A., 1980. A simple and effective pipe elbow element – linear analysis. J. Appl. Mech. 47, 93–100.

Bathe, k.J., Almedia, C.A., 1982. A simple and effective pipe elbow element – interaction effects. J. Appl. Mech. 49, 165–171.

Bathe, k.J., Almedia, C.A., Ho, L.W., 1983. A simple and effective pipe elbow element – some nonlinear capabilities. Comput. Struct. 17 (5–6), 659–667.

Baron, M.L., Matthews, A.T., 1961. Diffraction of a pressure wave by a cylindrical cavity in a elastic medium. J. Appl. Mech. (September), 347–354.

Brebbia, C.A., Dominguez, J., 1989. Boundary Element An Introductory Course. Computational Mechanics Publications, Southampton/Boston.

Cao, H., Lee, V.W, 1990. Scattering and diffraction of plane P waves by circular cylindrical canyons with variable depth-to-width ratio. Int. J. Soil Dynam. Earthquake Eng. 9 (3), 141–150.

Datta, S.K., Shah, A.H., 1982. Scattering of SH-waves by embedded cavities. Wave Motion 4, 256–283.

Dominguez, J., 1993. Boundary Elements in Dynamics. Computational Mechanics Publications, Southampton/Boston.

EL-Akily, N., Datta, S.K., 1980. Response of a circular cylindrical shell to disturbance in half-space. Earthquake Eng. Struct. Dynam. 8, 469–477.

EL-Akily, N., Datta, S.K., 1981. Response of a circular cylindrical shell to disturbance in half-space-numerical results. Earthquake Eng. Struct. Dynam. 9, 477–487.

Hwang, R.N., Lysmer, J., 1981. Response of buried structures to travelling waves. J. Geotech. Eng. Div., ASCE 107, 183–200.

Hashash, Y.M.A., Hooka, J.J., Schmidt, B., Yao, J.I.-C., 2001. Seismic design and analysis of underground structures. Tunnell. Underground Space Technol. 16, 247–293.

Khair, K.R., Datta, S.K., Shah, A.H., 1989. Amplification of obliquely incident seismic waves by cylindrical alluvial valleys of arbitary cross-sectional shape, Pt. I: Incident P and SV waves. Bull. Seismol. Soc. Am. 79, 610–630.

Kontoni, D.P.N, Beskos, D.E., Manolis, G.D., 1987. Uniform half-plane elastodynamic problems by an approximate boundary element method. Soil Dynam. Earthquake Eng. 6 (4), 227–238.

Kim, D.S., Konagai, K., 2000. Seismic isolation effect of a tunnel covered with coating material. Tunnell. Underground Space Technol. 15 (4), 437–443.

Karl, J., Lee, V.W., 1991. Scattering and diffraction of elastic waves by an underground, circular cylindrical tunnel (cavity). Civil Engineering Report No. CE91-04, University of Southern California, Los Angeles.

Luco, J.E., De Barros, F.C.P., 1994. Dynamic displacement and stress in the vicinity of a cylindrical cavity embedded in half space. Earthquake Eng. Struct. Dynam. 23, 321–340.

Lee, V.W., 1977. On deformation near circular underground cavity subjected to incident SH-waves. In: Proc. Symp. on Application of Computer Methods in Engineering, August 23–26. University of Southern California, Los Angeles, pp. 951–962.

Lee, V.W., Trifunace, M.D., 1979. Response of tunnels to incident SH-waves. J. Eng. Mech. Div., ASCE 105, 643–659.

Lee, V.W., Cao, H., 1989. Diffraction SV waves by circular cylindrical canyons of various depths. ASCE., Eng. Mech. Div. 115 (9), 2035–2056.

Lee, V.W., Karl, J., 1992. Diffraction of SV waves by underground circular cylindrical cavities. Int. J. Soil Dynam. Earthquake Eng. (8), 445–456.

Lee, V.W., Karl, J., 1993. Diffraction of Elastic P Waves by Circular, underground and unlined tunnels, Eur. Earthquake Eng.

Liu, S.W., Datta, S.K., Bouden, M., 1991. Scattering of obliquely incident seismic waves by a cylindrical valley in a layered half-space. Earthquake Eng. Struct. Dynam. 20, 859–870.

Moore, I.D., Guan, F., 1996. Three-dimensional dynamic response of lined tunnels due to incident seismic waves. Earthquake Eng. Struct. Dynam. 25, 357–369.

Manolis, G.D., Beskose, D.E., 1988. Boundary Element Methods in Elastodynamics. Unwin Hymanm, London.

Oden, J.T., Ripperger, E.A., 1981. Mechanics of Elastic Structures, second ed. McGraw-Hill Book Company.

Pao, Y.H., Maw, C.C., 1973. Diffraction of Elastic Waves in Dynamic Stress Concentrations. Crane Russake, New York.

Stamos, A.A., Beskos, D.E., 1996. 3-D seismic response analysis of long lined tunnels in half-space. Soil Dynam. Earthquake Eng. 16, 111–118.

Shah, A.H., Wong, K.C., Datta, S.K., 1982. Diffraction of plane SH-waves in a half space. Earthquake Eng. Struct. Dynam. 10, 519–528.

Shah, A.H., Wong, K.C., Datta, S.K., 1983. Single and multiple scattering of elastic waves in two dimensions. J. Acoust. Soc. Am. 74, 1033–1043.

St. John, C.M., Zahara, T.F., 1987. A seismic design of underground Structures. Tunnell. Underground Space Technol. 2 (2), 165–197.

Vahdani, S.H., 1982. On finite elements of the pipe elbow structures, Ph.D. Thesis, Faculty of The Graduate School, University of Southern California.

Wong, K.C., Shah, A.H., Datta, S.K., 1985. Diffraction of elastic waves in half-space. II. Analytical and numerical solutions. Bull. Seismol. Soc. Am. 75, 69–92.

Wang, J.N., 1993. Sesimic Design of Tunnels: A State-of-the-Art Approach, monograph 7. Parsons, Brinckerhoff, Quade and Douglas Inc, New York.

Zhang, L.P., Chopa, A.K., 1991. Computation of spatially varying ground motion and foundation-rock impedance matrices for seismic analysis of arch dams. Report No. UCB/EERC-91/06, University of California, Berkeley, CA.

Zhang, L.P., Chopa, A.K., 1991b. Three-dimensional analysis of spatially varying ground motions around a uniform canyon in a homogenous half-space. Earthquake Eng. Struct. Dynam. 20, 91–126.

Zhang, L.P., Chopa, A.K., 1991c. Impedance functions for three-dimensional foundations supported on an infinitely-long canyon of uniform cross-section in a homogeneous half space. Earthquake Eng. Struct. Dynam. 24, 1711–1720.